Medical Engineering and Physics 69 (2019) 72–84

Contents lists available at ScienceDirect

Medical Engineering and Physics

journal homepage: www.elsevier.com/locate/medengphy

Experimental methodology for quantitative assessment of heat-wrap thermal transient behavior

Paolo E. Santangelo*, Giulia Santunione, Alberto Muscio

Dipartimento di Ingegneria "Enzo Ferrari", Università degli Studi di Modena e Reggio Emilia, Via P. Vivarelli 10, 41125 Modena, Italy

ARTICLE INFO

Article history:
Received 2 January 2019
Revised 4 April 2019
Accepted 13 May 2019

Keywords:
Pain management
Heat transfer modes
Thermometry
Infrared thermography
Test procedure

ABSTRACT

Among the numerous thermotherapy methods, heat wraps have been largely used over the last 2 decades as a self-administered practice for pain relief. Therefore, understanding their performance has become instrumental within the healthcare industry. However, the majority of the available studies have been focused on *in vivo* clinical performance, whereas a standardized, quantitative approach to evaluate and compare the various heat-wrap types against each other is lacking. An experimental methodology is proposed to carry out a comparative assessment between heat wraps in terms of their transient thermal behavior. A simple setup was developed to measure wrap/substrate interface temperature trend. The approach was validated by a preliminary infrared-thermography assessment and statistical analysis on the extensive dataset acquired on commercial heat-wrap types for low-back and neck pain relief. The heat-release trend was found to be qualitatively similar over all the investigated types, consisting of rapid growth, stationary phase, decay and end of the reactions. A set of parameters is also proposed to summarize heat-wrap thermal performance.

1. Introduction

Low back pain (LBP) and neck pain (NP) have been identified as some of the most widespread health problems in industrialized countries and, when persistent, major causes of disability [1,2]. LBP and NP have a lifetime prevalence over the world population in the range of 60%–70% and 14%–71%, respectively [3,4]. Approximately 50% of working-age individuals in the United States report LBP or NP symptoms each year. As a result of their high epidemiologic incidence, LBP and NP economic impact on annual societal costs was estimated in the range 20,000 – 50,000 M$ in USA and about 15 M€ in Europe [1,5]. Productivity loss due to forced bed rest takes the largest share of these costs [6–8]. So, developing and selecting the most effective clinical strategies for that soreness is currently instrumental.

Both pharmacologic and non-pharmacologic treatments are currently available for LBP and NP. Drugs are often advocated as a first-line treatment for acute episodes, but their efficacy is questioned [9] and side effects may arise [10,11]. Among non-pharmacologic strategies, manipulation and mobilization, bed rest, bracing and heat therapy – also known as thermotherapy – are the most employed [12]. Heat therapy is arguably the most common treatment to facilitate tissue healing [13–15]. Within thermotherapy, heat wraps represent a self-administered practice to manage the first acute phase of LPB and NP. These medical devices are based on chemical and physical principles, since they rely upon air-activated chemical warmers (e.g., powdered iron, sodium chloride, charcoal) enclosed within oxygen-permeable cells or pockets. As the wrap is exposed to air, oxygen diffuses through the wrap outer layer – typically a porous fabric – and reaches the cells, thus starting an exothermic oxidation reaction with the reactant available inside. As a result, products as iron oxide are generated together with heat [16]. The open literature reports conflicting outcomes on heat-wrap efficacy: Shaheed et al. [17] found no immediate evidence of analgesic effect; other works suggest that application of heat onto the skin surface yields pain relief, decreases local muscle spasms and reduces disability rate [12,18–21]. Most of, if not all, the available studies on heat therapy describe *in vivo* performance and clinical significance [18–20,22–25], thus emphasizing a general lack of solid, quantitative approaches to assess and compare heat-wrap thermal transient trend. Notably, *in vivo* investigations are inherently related to patients' clinical conditions, which include the type of pain they endure (e.g., lumbar, neck, knee) and their physiological status with the associated variability.

The present work is aimed at proposing a robust experimental methodology to identify quantitatively the physical mechanisms underlying heat-wrap performance. Their thermal behavior is the specific target of the developed approach towards a test protocol

* Corresponding author.
E-mail address: paoloemilio.santangelo@unimore.it (P.E. Santangelo).

https://doi.org/10.1016/j.medengphy.2019.05.003
1350-4533/

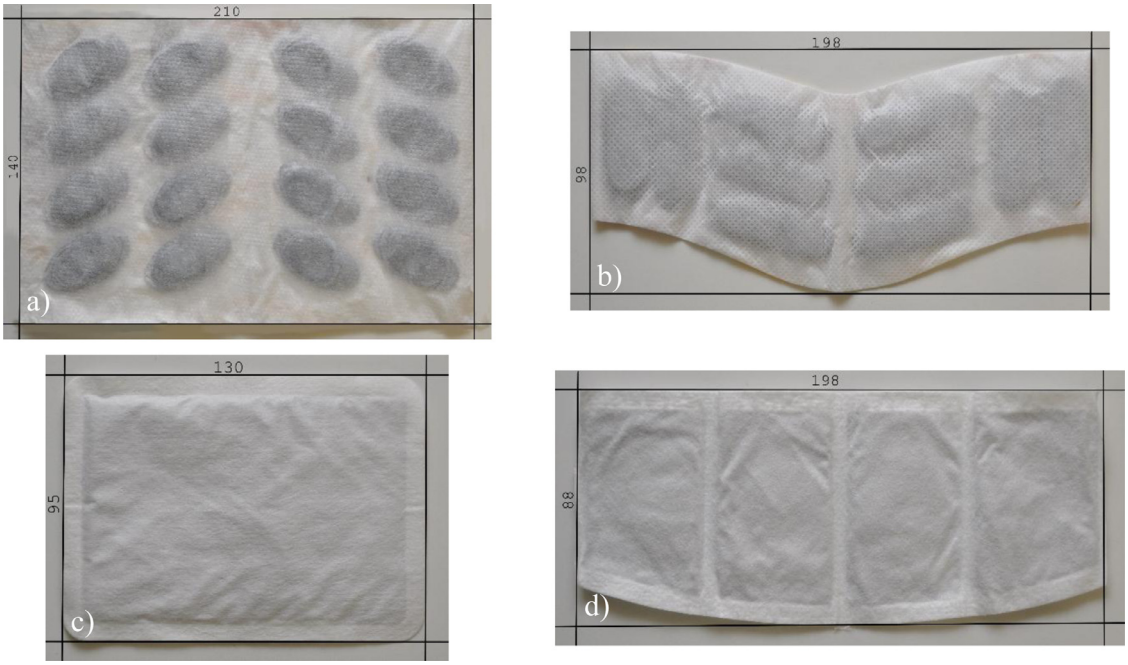

Fig. 1. Shape and characteristic dimensions of the tested heat-wrap types: (a) A_b; (b) A_n; (c) B_b; (d) B_n (dimensions are in mm).

for comparing different heat-wrap types. Moreover, acquiring an extensive dataset on commercial heat wraps for LBP and NP relief was deemed necessary to support the proposed method. Ultimately, this research embodies an unprecedented effort that benefits from background and techniques typical of the engineering field.

Interdisciplinary approaches have shown remarkable effectiveness in medical innovation [26–29]. Notably, the role of engineering has grown dramatically since the early 80 s, yielding early detection of health problems, accurate diagnostic instruments and sharp response to patients' needs. There is an extensive history of thermophysics concepts applied to develop medical devices and methods, among which infrared thermography is recognized as a key non-intrusive and non-radiating tool [29]. A physical investigation of the heat-wrap thermal behavior was carried out employing techniques and instruments typical of thermofluid engineering within a self-developed test setup, providing significant information on heat-wrap life dynamics and devising a standard test method to assess their performance. Heat-wraps manufacturers and medical specialists dealing with musculoskeletal disorders can benefit from both the findings and the methodology, which also serves as a reference to evaluate future product improvements.

2. Materials and methods

An experimental setup was developed to investigate quantitatively heat-wrap thermal behavior from opening of the sealed package (i.e., start of the reactions) to the complete conversion of the available chemical warmer. The test facility is aimed at reproducing boundary conditions consistent with those occurring when a heat wrap is applied onto the body surface; that refers specifically to wall temperatures (first-type boundary condition [30–32]) and amount of oxygen made available around the wrap for diffusion and reaction. The apparatus was made as simple as possible to emphasize robustness and ability to compare heat-wrap performance with no or very limited influence of ambient conditions, the fluctuations of which during each test and between tests may reduce their consistency.

The experimental setup consists of multiple test assemblies capable of hosting several heat-wrap samples to be tested in parallel. Four commercial products were analyzed: 2 brands (A and B), each of which sells heat wraps for LBP and NP treatment, identified by subscript b and n respectively. The shape and characteristic dimensions of the tested heat-wrap types are reported in Figure 1. Three different batches were selected for each heat-wrap type and 5 samples were tested for each batch to allow building a substantial dataset for statistical analysis towards an assessment of repeatability.

2.1. Ambient conditions

Evaluating and comparing the thermal transient characteristics of a solid surface in direct contact with a heat wrap implies that ambient temperature and relative humidity be kept as constant and steady as possible throughout each experiment and over the whole experimental campaign. All tests were carried out in a controlled room, where air nominal relative humidity (RH) and temperature (T_{room}) were monitored; suitable devices – an electric heater and a humidifier with embedded control systems – were inserted to allow continuous automatic adjustment to the imposed values of ambient temperature and humidity. Notably, an electrical heater was employed to maintain T_{room} at 20 ± 2 °C; a humidifier loaded with distilled water was operated under a relative-humidity setting of 40% ± 5%. Since tests were run at ambient pressure not lower than 0.98 bar (a common value that excludes extreme altitudes), water-vapor partial pressure resulting from those conditions was higher than 0.9 kPa [33], which translates into vapor quality typical of indoor configurations [34].

2.2. Experimental setup

The developed facility consists of a number of parts and instruments (Fig. 2). Firstly, a radiant barrier – a solid plate, the temperature of which is close to that of the air in close proximity to the test region, rather than to that of the chamber ceiling – is conveniently placed above the test region, between tested samples and ceiling (Fig. 2a). A flat sample lying horizontally would exchange

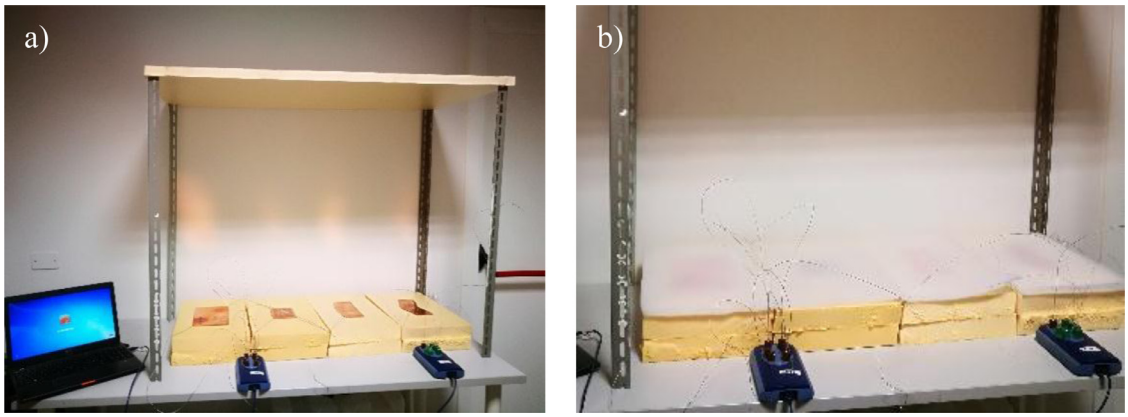

Fig. 2. (a) View of the setup with the polystyrene radiant barrier (on top), 4 test stations (100 mm thick insulating layer with the copper foil) and with 2 loggers for thermocouples; (b) setup with the 10 mm thick polyester filter placed onto copper foils and insulating layers.

heat mostly with the ceiling (horizontal as well); radiative transfer with other unshielded vertical surfaces may occur, but to a smaller extent as a result of lower view factors. The larger and closer to the tested sample the radiant barrier, the lower radiation heat transfer between sample and the surrounding surfaces, provided that sufficient space be allowed to perform test operations. The absence of a barrier does not imply failed experiments, yet it impacts on the operative temperature [35] accounting for radiative and convective contributions: the former may be an issue as the experiment is reproduced in different rooms and, even if reasonably constant within the same chamber, quantifying it can be challenging. So, a polystyrene panel held by a steel frame was used as the radiant barrier.

An insulating layer (Figs. 2a and 2b) was placed onto the holder supporting the test rig; it consists of a series of polystyrene (30 kg m^{-3} density and 0.035 W m^{-1} K^{-1} thermal conductivity) panels yielding a total thickness of 100 ± 2 mm. Insulation allows keeping very low – practically negligible – and relatively constant downward heat flow.

A highly conductive foil made of 0.5 mm thick copper (99.95% – 99.98% pure copper) was placed onto the insulating layer (Fig. 2a), being its thermal conductivity close to that of 99.9% pure copper (385 W m^{-1} K^{-1} [36]). Original foils were cut to form surfaces as coincident as possible with those of the investigated heat-wrap types, in order to host heat wraps onto them with the sharpest contact between the 2 surfaces. The foil center of mass was set at the same axial location of that of the insulating layer for the sake of symmetry. The insulating-layer rectangular top surface was cut to an area 4 times that of the rectangle into which the foil surface is inscribed. Copper foils provide a fast heat-transfer rate both along the axial direction and over the wrap/foil interface surface as a result of copper high thermal conductivity, yielding a rather homogeneous surface temperature at the heat-wrap bottom surface, the one in contact with body skin in actual applications. So, the chosen foils allow considering the foil bottom surface at the same temperature of the upper (interface) surface. As heat wraps are often made of cell arrays or consist of pockets with uneven thickness, the heat-rate spatial distribution may be uneven over the interface surface. However, the temperature homogeneousness over the foil bottom surface makes temperature measurements taken over it virtually independent of the location and become an indirect estimate of the average heat flow rate transmitted from the heat wrap to the body surface. In a similar manner, blood circulation is expected to cause a comparable heat spread.

Each foil was instrumented with 3 thermocouples taped to its bottom surface to measure temperature trend at 3 different locations. These locations are shown in Figure 3 for a generic foil shape: the first one corresponds to the center of mass of the foil; the rectangle into which the foil surface is inscribed has 2 diagonals, so 4 more locations are identified as those corresponding to half the length of each semi-diagonal from the center of mass. Only 2 of those 4 locations were chosen as sampling points, one opposite to the other with respect to the center of mass over the same diagonal. K-type (0.5 mm wire diameter) and T-type (1 mm wire diameter) thermocouples (accuracy: ±0.75% of the reading, according to standard IEC 60 584-2:1995) were employed in this work. Very thin channels were engraved into the insulating layer top surface to host thermocouple wires connecting the bead to the Data Acquisition system. The channel diameter was made sufficiently small that the local heat transfer between copper foil and insulation layer was not affected significantly.

Heat wraps were placed onto the foil with their active surface against the foil upper surface. A 10 mm thick polyester fibrous layer was placed onto the heat-wrap upper surface (Fig. 2b). This layer serves as a porous thermal interface; its thermal conductivity was measured by a guarded hot-plate apparatus as equal to 0.047 W m^{-1} K^{-1} (±10% uncertainty). Its level of filtration is G3, with pressure drop lower than 70 Pa at flow-through air velocity lower than 1.5 m s^{-1} (complying with standards ISO 9073-2 and EN779:2012). The insulating layer made the upward heat flow govern heat-wrap thermal behavior; the porous thermal interface made the resistance to heat flow between the wrap upper surface and the ambient air increase by an order of magnitude, otherwise the heat flow would have been driven by convection and radiation. However, the interface shall not prevent oxygen and water vapor contained in ambient air from reaching the wrap outer layer and starting chemo-physical reactions. Some preliminary analyses with larger (20 and 30 mm) and smaller (null) thickness of the fibrous layer showed that its barrier to reacting oxygen flow does not affect the heat-wrap thermal behavior. A thickness as low as 10 mm was chosen to not modify significantly the heat-wrap upper surface temperature from its typical operative value. Such settings yield a thermal resistance by the porous interface smaller than that of the insulating layer by more than an order of magnitude. Overall, the proposed configuration generates a heat flow rate from heat wraps consistent with that actually transferred through the body surface and added to metabolic heat by superposition principle [28,37]. Figure 4 shows the flow chart to assemble a generic test station.

Two additional thermocouples were inserted to record T_{room}, one being oriented towards the center of the test rig under the radiant barrier and the other towards the center of the chamber. Two data loggers by Pico Technology were employed and 2 probes by EasyLog (±10% accuracy) were also added to record relative

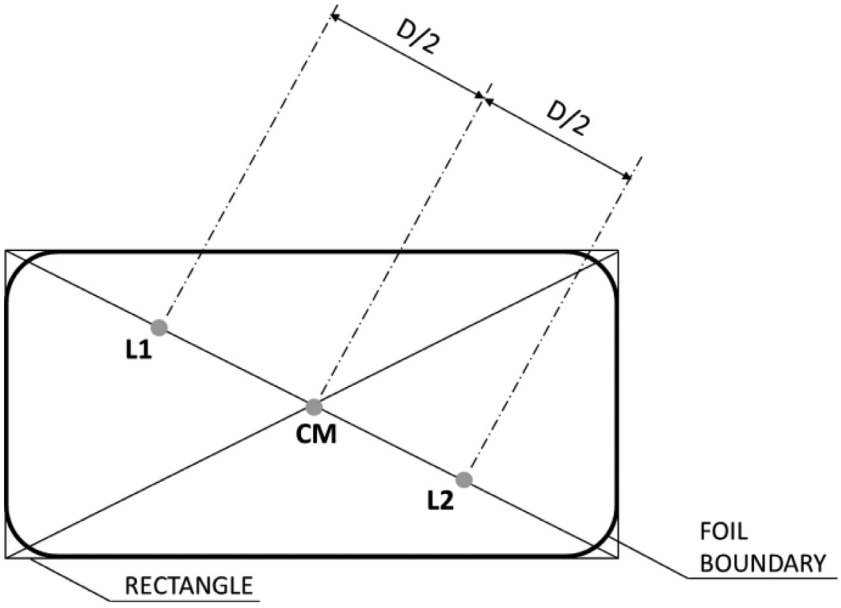

Fig. 3. Sketch of a simple foil geometry with the sampling locations for temperature probes; *CM*: center of mass; *L1, L2*: possible locations over one of the diagonals; *D*: semi-diagonal length.

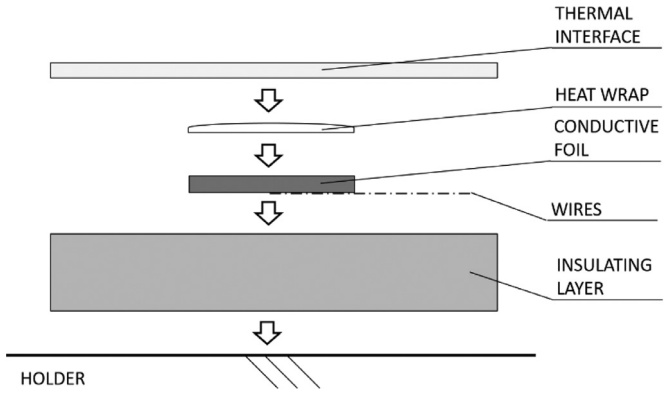

Fig. 4. Procedure for assembling the setup.

humidity, one of which positioned in the test rig close to the sampling region and the other at the center of the test chamber.

2.3. Preliminary tests

Some preliminary tests were run in order to assess some design parameters and to evaluate some of the features expected by the components.

The first test was performed to investigate polystyrene insulating capability. Two different thickness values were considered: 50 and 100 mm. To this end, a K-type thermocouple was inserted between the bottom surface of the insulating layer and the holder. The comparison between temperature signatures in the 2 configurations allowed identifying the most effective thickness, marked by an insulating layer/holder interface temperature close or equal to the ambient. These tests were carried out on the same heat-wrap type at 40% nominal *RH* and 20 °C T_{room}. As shown in Figure 5a, the interface temperature recorded in the case with a 50 mm thick insulating layer is mildly higher than T_{room} during most of the heat-wrap life time (3.5 °C maximum temperature difference). On the other hand, the interface temperature profile for the case with a 100 mm thick insulating layer almost collapses onto the T_{room} trend (Fig. 5b), the maximum temperature difference (1.6 °C) almost falling into thermocouple uncertainty range. So, a 100 mm thick polystyrene layer performs well, whereas a 50 mm thickness yields a slightly less than perfect insulation.

A second test was conducted to evaluate a possible effect of *RH* against heat-wrap heat release, possibly due to an influence on reaction kinetics. To this end, 2 tests were run at 40% and 80% *RH* against the same heat-wrap type, being T_{room} kept constant at 20 °C. No significant variation in temperature profiles of the foil bottom surface was observed between the 2 tests, which suggests that nominal *RH* does not impact on thermal behavior of the investigated heat wraps, provided that water-vapor partial pressure in ambient air be kept consistent with the conditions suggested in Sub-Section 2.1.

The performance of the highly conductive material as a heat spreader was also assessed. The temperature uniformity over the copper-foil bottom surface was examined for a representative heat wrap: it features discrete cells containing chemical warmers, so the heat-flow distribution may be spatially uneven. An infrared thermocamera (T640 by FLIR Systems, 640 × 480 pixels uncooled InfraRed – Long Wave detector type, Noise Equivalent Temperature Difference < 0.035 °C) was employed to evaluate foil surface temperature. The heat-wrap was attached to the foil upper surface. The foil bottom surface had been previously black-painted to increase its emissivity and allow setting it as 0.9 in image post-processing, as in several previous studies [38–44]. The thermocamera was focused on the black-painted bottom surface, while the heat wrap was operating and heated the foil upper surface. Thermographic images were taken at various times throughout the thermal transient evolution. The copper foil with the attached heat wrap was held at its borders and kept immersed in ambient quiescent air, so temperature values measured in these experiments may not be considered representative of actual contact temperature. Thermograms are shown at 1 h (Figs. 6a and 6b) and 7 h (Figs. 6c and 6d) after wrap deposition, with a relatively large temperature range applied to temperature maps of Figures 6a and 6c, and a narrower range (3 °C) applied to maps of Figures 6b and 6d. The maximum detected temperature gap between different zones of the surface below the heat wrap was lower in the order of 0.5 °C. So, the thermographic analysis demonstrated that copper foils act as heat spreaders, thus ensuring a relatively homogeneous

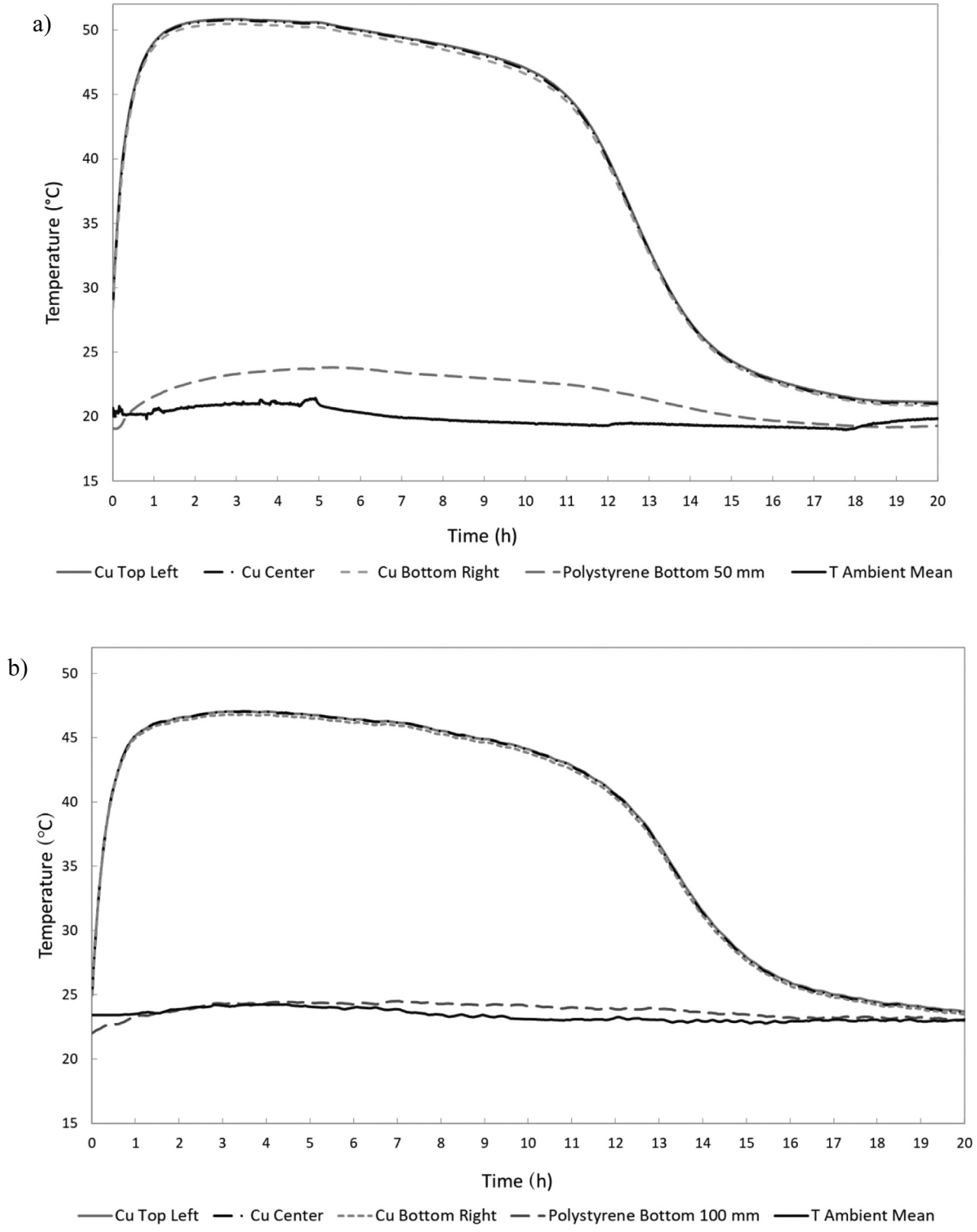

Fig. 5. Temperature signature for the 3 thermocouples on the foil-bottom surface (*Cu*: copper foil; *Top Left, Center, Bottom Right*: locations on the surface), mean room temperature (*Ambient Mean*) and at the insulating layer/holder interface (*Polystyrene Bottom* 50 mm and *Polystyrene Bottom* 100 mm): (a) case with 50 mm thick insulating layer; (b) case with 100 mm thick insulating layer.

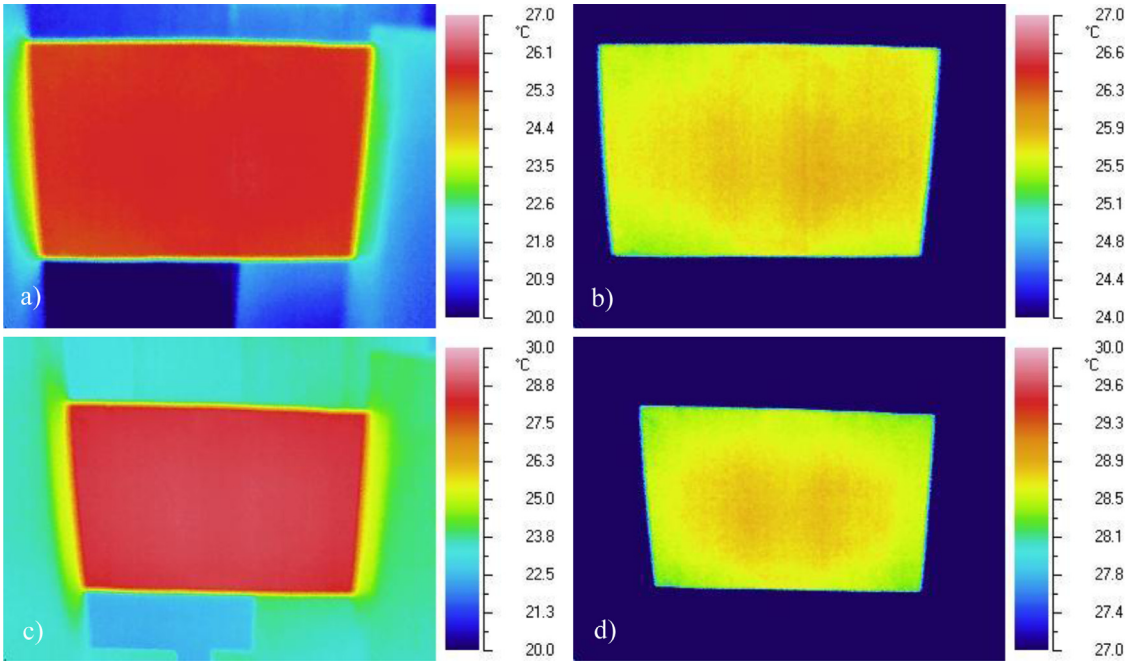

Fig. 6. Thermograms of the copper-foil bottom surface: (a) 1 h after heat-wrap deposition (large temperature range); (b) 1 h after heat-wrap deposition (narrow temperature range); (c) 7 h after heat-wrap deposition (large temperature range); (d) 7 h after heat-wrap deposition (narrow temperature range).

temperature distribution over the sampling surface. Moreover, a homogeneous contact between heat wrap and copper-foil surface can be achieved and, most importantly, the heat release from the heat wrap also appears spatially homogeneous.

2.4. Experimental procedure and data analysis

Before starting each experiment, the 2 *RH* probes were positioned in the test chamber, reasonably far away from possible sources of bias (e.g., door, humidifier). The sealed packages were opened thereafter to allow chemical reactions with oxygen to start. Heat wraps were deposited onto the upper foil surface, with the 2 surfaces made as co-planar and coincident as possible. The porous thermal interface was then placed onto the heat-wrap upper surface and the exposed insulating layer surface around it.

Data recording and acquisition was started simultaneously for temperature and *RH* readings. Acquisition frequency was set at 1/15 s^{-1} for thermocouples and 1/60 s^{-1} for *RH* probes. The total experimental time was varied between 20 and 24 h, based on the duration of the last phase upon ending of the reactions. Most manufacturers claim a shorter active time (about 8 h), probably identifying the time during which patients experience most physiological benefits.

Data analysis started from mean ambient temperature $T_{mean,room}$ and foil surface temperature T. $T_{mean,room}$ is actually a function of time t and the following formula was applied to calculate $T_{mean,room}$ at each acquisition:

$$T_{mean,room} = \frac{\sum_i T_{room,i}}{n}, \tag{1}$$

where i refers to the ith reading from the ith probe and n is the total number of thermocouples dedicated to record T_{room} ($n = 2$ in the present tests). Since the comparison between heat wraps practically consists of comparing foil bottom-surface temperature, the temperature difference ΔT between those readings and mean ambient temperature was computed to offset the effect of ambient conditions for each acquisition at each sampling location:

$$\Delta T_j = T_{foil/wrap,j} - T_{mean,room}, \tag{2}$$

where j refers to the jth sampling location and $T_{foil/wrap}$ is the corresponding temperature reading. It is noteworthy to mention that Eq. (2) applies as the experimental setup was placed under the radiant barrier. If no radiant barrier were used, the operative temperature T_{op} – defined as *"a uniform temperature of an imaginary black enclosure in which an occupant would exchange the same amount of heat by radiation plus convection as in the actual nonuniform environment"* [35] – should be calculated at each acquisition time employing $T_{mean,room}$ as the air temperature and following the formulation provided in [35]. ΔT should be finally calculated, inserting T_{op} instead of $T_{mean,room}$ into Eq. (2). That strengthens the recommendation to use a radiant barrier, since that makes ambient temperature practically equal to T_{op}. This assumption was also verified through a preliminary comparison of ambient temperature recorded by thermocouples with temperature recorded by a globe thermometer measuring T_{op}.

Assuming a function $T = T(t)$ for the wrap/foil interface, its first derivative allows a quantitative discussion of its trend. It can be expressed through an approximation over the acquisition series [45,46]:

$$T'(t) = \frac{dT}{dt} \approx \frac{T_k - T_{k-1}}{\Delta t} = \frac{T_k - T_{k-1}}{1/f}, \tag{3}$$

where k refers to the kth acquisition (with the series of k starting with 1) and f is acquisition frequency, if employed for the calculation. Eq. (3) was applied to all the 3 sampling locations.

Statistical analysis was performed as an assessment of repeatability through Analysis Of Variance (ANOVA) method [47]. ANOVA quantifies the relative size of variance among group means, the "between group variance" s_b^2, to be compared with the average variance within groups, the "within group variance" s_w^2; those quantities are expressed as follows:

Table 1
Mean values of ambient temperature and relative humidity referred to all performed test sessions; min: minimum, max: maximum.

	$T_{room,min}$ (°C)	$T_{room,max}$ (°C)	RH_{min} (%)	RH_{max} (%)
Mean M	18.54	21.39	40.53	46.25
Standard deviation SD	0.61	0.48	2.96	1.80

$$s_b^2 = \sum_{i=1}^{n_j} n_j \left(\overline{x_{ij}} - \overline{X}\right)^2, \tag{4}$$

$$s_w^2 = \sum_{j=i}^{k} \sum_{i=1}^{n_j} \left(x_{ij} - \overline{x_{ij}}\right)^2, \tag{5}$$

where k is the number of groups (i.e., the 3 batches), n is the number of observations (i.e., 5 heat wraps per each batch), x_{ij} identifies each observation, $\overline{x_{ij}}$ is the mean value over the single group, $\bar{X}$ is the overall mean of x_{ij} and i and j are indexes within observations and groups respectively. The s_b^2/s_w^2 ratio is evaluated by ANOVA and represents the F-value of F-distribution [48]. The calculated F-value is then compared with a F-critical value that depends on the degrees of freedom according to the chosen error level α. If the calculated F-value is lower than or the same as F-critical, the difference between and within the considered groups is assumed as not statistically significant (the Null Hypothesis H_0). The chosen α value indicates the level of significance (p-value) of the results; the probability p of finding the observed results when H_0 is verified is yielded by:

$$p = 1 - \alpha. \tag{6}$$

As an additional task within statistical analysis, 2 operators – mean value M and standard deviation SD – were applied to the dataset of parameters representative of both ambient conditions and heat-wrap performance, according to recognized formulations [49].

3. Results

Heat-wrap thermal transient behavior was investigated over a total of 60 wraps (5 samples × 3 batches × 2 types × 2 brands): 2 brands (A and B), one type for LBP treatment (A_b and B_b) and one for NP treatment (A_n and B_n). Mean ambient conditions over the whole experimental campaign are reported in Table 1. The relatively low SD values for T_{room} and RH allow considering ambient conditions almost constant through all the tests.

The comparison between A_b and B_b heat-wrap types in terms of average foil surface temperature is shown in Figure 7a: the mean value of the 3 readings at all sampling locations was calculated for every acquisition; time 0 was set at the start of data acquisition. As an additional insight into transient heat transfer at the wrap/foil interface, the first-derivative trend is also presented in Figure 7b for the same types. The profiles exhibit 4 different and distinct phases throughout heat-wrap lifetime. The first phase is characterized by a rapid temperature growth with $T'(t) > 10^{-5}$ °C s^{-1} and lasts until $T'(t)$ becomes lower than 10^{-5} °C s^{-1} . A relatively stationary phase occurs thereafter, which features different duration for A_b (Fig. 7a) and B_b (Fig. 7b) types: it runs mostly over the range $-10^{-5} < T'(t) < 10^{-5}$ °C s^{-1} and ends as a fast temperature decrease (third phase) takes place with $T'(t) < -10^{-5}$ °C s^{-1}. The stationary phase lasts longer for B_b than A_b; the phase with declining slope occurs by a more rapid decrease for A_b, which reaches the last phase earlier than B_b type. The last section of heat-wrap lifetime starts as $T'(t)$ falls again in the range $-10^{-5} < T'(t) < 10^{-5}$ °C s^{-1}: reactions are ended and the heat-wrap temperature decays asymptotically to T_{room}. Regardless of duration, temperature and first-derivative values, the exhibited overall behavior is common to all the tested heat-wrap types and its evidence was captured in all the experiments. The approach to the calculation of first derivative of temperature is clarified in Figure 7c, where its trend through the growth phase of A_b type is shown as calculated with 3 different values for Δt: 15 s (= 1/f), 60 s and 120 s. The 2 latter cases implied to reformulate Eq. (3) by inserting the temperature difference between the reading at $\Delta t/2$ after the kth acquisition and the reading at $\Delta t/2$ after the kth acquisition in the numerator. Figure 7c shows that high acquisition frequencies produce noisy datasets, whereas employing larger Δt in the calculation may yield a smoother curve, without biasing the actual trend. To this end, 120 s was found a significant timeframe, so it was used to calculate the dataset shown in Figure 7b.

ΔT trends are presented in Figure 8. The 5 curves for each batch show the average ΔT over the 3 sampling locations at the foil bottom surface per every acquisition. From the same dataset, 2 parameters representative of heat-wrap overall thermal trend could be defined and calculated: t_{max} is the time from the start of acquisition to reach the maximum temperature (T_{max}) and is a measure of duration of the initial growth phase; an assessment of the effective heat-wrap life consists of the time to reach t_{max} after t_{max}, referred to as effective time (t_{eff}).

Some differences between heat-wrap types for both LBP and NP treatment were found. As for the former (Fig. 8a), the achieved ΔT_{max} (maximum ΔT) by the 2 brands is very close and occurred over the stationary phase: 24.6 ± 0.7 °C for A types and 24.6 ± 0.5 °C for B types. However, the former reached T_{max} after about 2.7 h, whereas the latter did after 5.5 h. An analysis of t_{eff} showed that heat-wrap lifetime seems on average longer for B types: 16.4 ± 0.6 h against 13.5 ± 0.6 h for A types. A similar, yet more emphasized transient behavior is exhibited by heat wraps for NP treatment (Fig. 8b). A type heat wraps achieve on average a higher ΔT_{max} than B types: 26.2 ± 0.5 °C against 19.6 ± 0.5 °C. Consistent with LBP treatment, A type samples are on average faster in achieving T_{max}, when compared with the mean value of B type samples: 2.1 ± 0.3 h against 4.1 ± 0.7 h. On the other hand, A type heat wraps present a remarkably shorter lifetime, embodied by t_{eff}: 10 ±0.3 h against 19.4 ± 0.3 h for B type.

4. Discussion

The obtained results highlight some differences in the thermal behavior between the tested heat-wrap brands. Figure 9 shows a comparison between representative heat wraps for LBP and NP treatment belonging to the same brand. While A type heat wraps exhibit a similar behavior for both kinds of treatment, a slightly higher variability can be observed among B type. As for the reliability of the proposed methodology, it is worth emphasizing the almost perfect overlapping of the curves related to the same heat-wrap type at the 3 sampling locations over the foil-bottom surface: in all the experiments, a maximum discrepancy lower than 2 °C was found between readings at different sampling locations for the same acquisition. Such a consistency – the difference falls within thermocouple uncertainty range – matches well the ability of the copper foil to act as a heat spreader, proven by infrared thermography tests. Therefore, the developed setup and methodology can be effectively applied to compare different heat wraps.

Tables 2 and 3 report the parameters of interest for each tested heat wrap, together with the results of statistical analysis applied to each batch. A significant difference in terms of t_{max} and t_{eff} can be observed between brands; that difference seems inherently related to heat-wrap geometry and physical configuration, since the low values of standard deviation and the consistency of mean values over the same type imply good repeatability. As for LBP

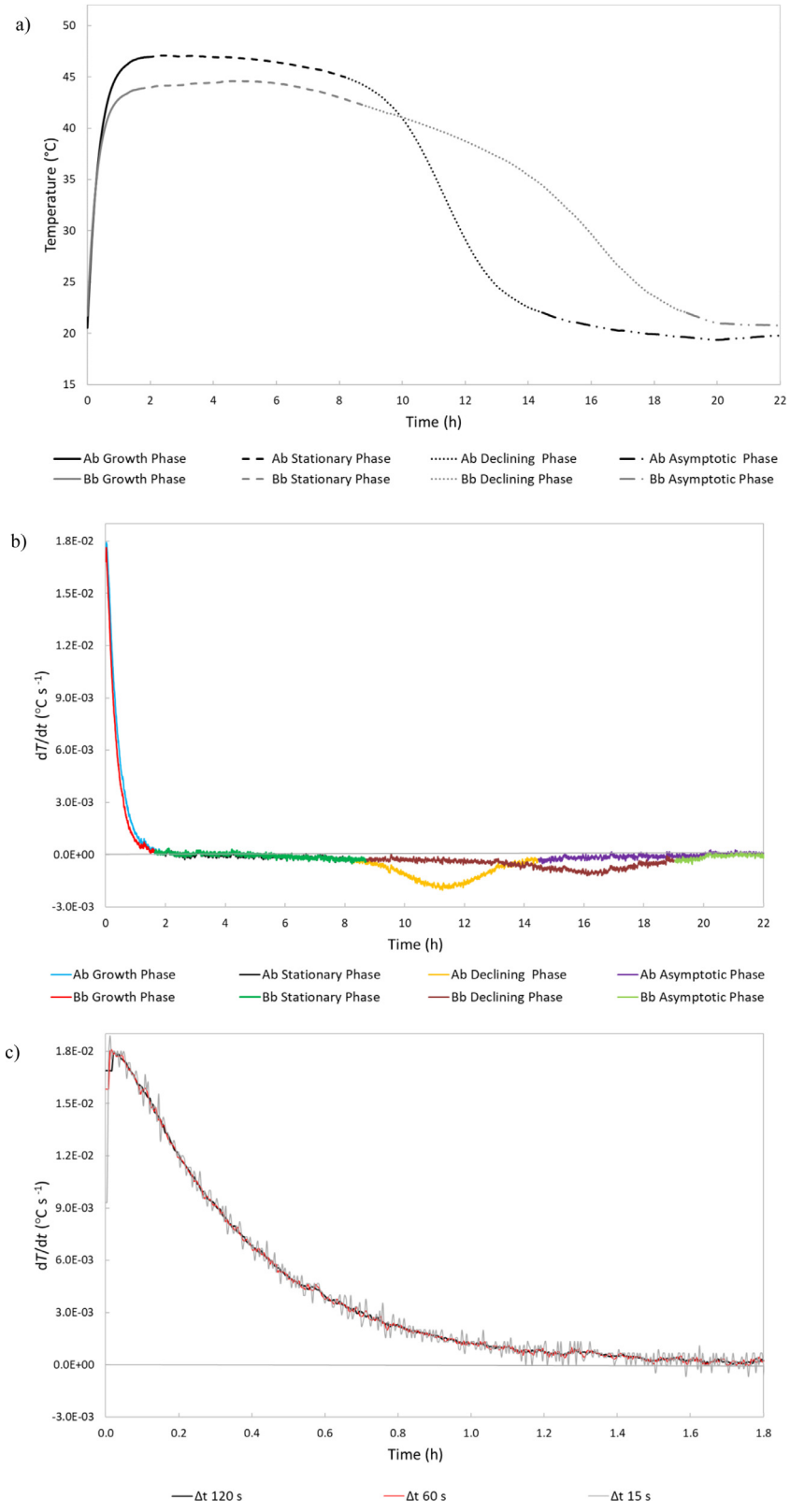

Fig. 7. (a) Trends of the foil-bottom surface average (mean value over the 3 sampling locations) temperature for A_b type and B_b type; (b) trends of first derivative of temperature for A_b type and B_b type; (c) first derivative of temperature through the growth phase for A_b type, calculated with 3 different Δt values.

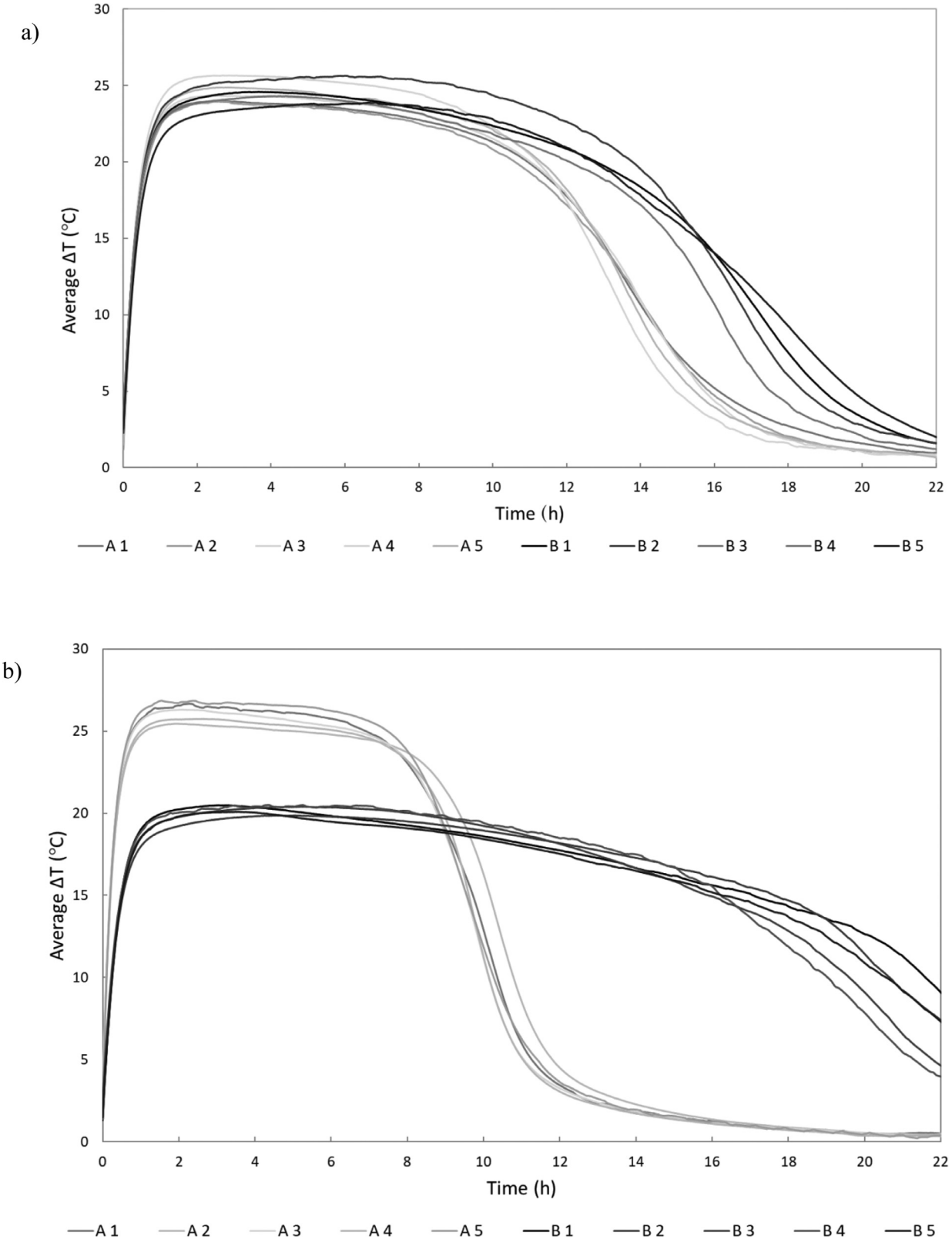

Fig. 8. Average foil-bottom surface temperature for each sample (5 in total) of a representative batch: (a) *A* and *B* type for LBP treatment (A_b and B_b); (b) *A* and *B* type for NP treatment (A_n and B_n).

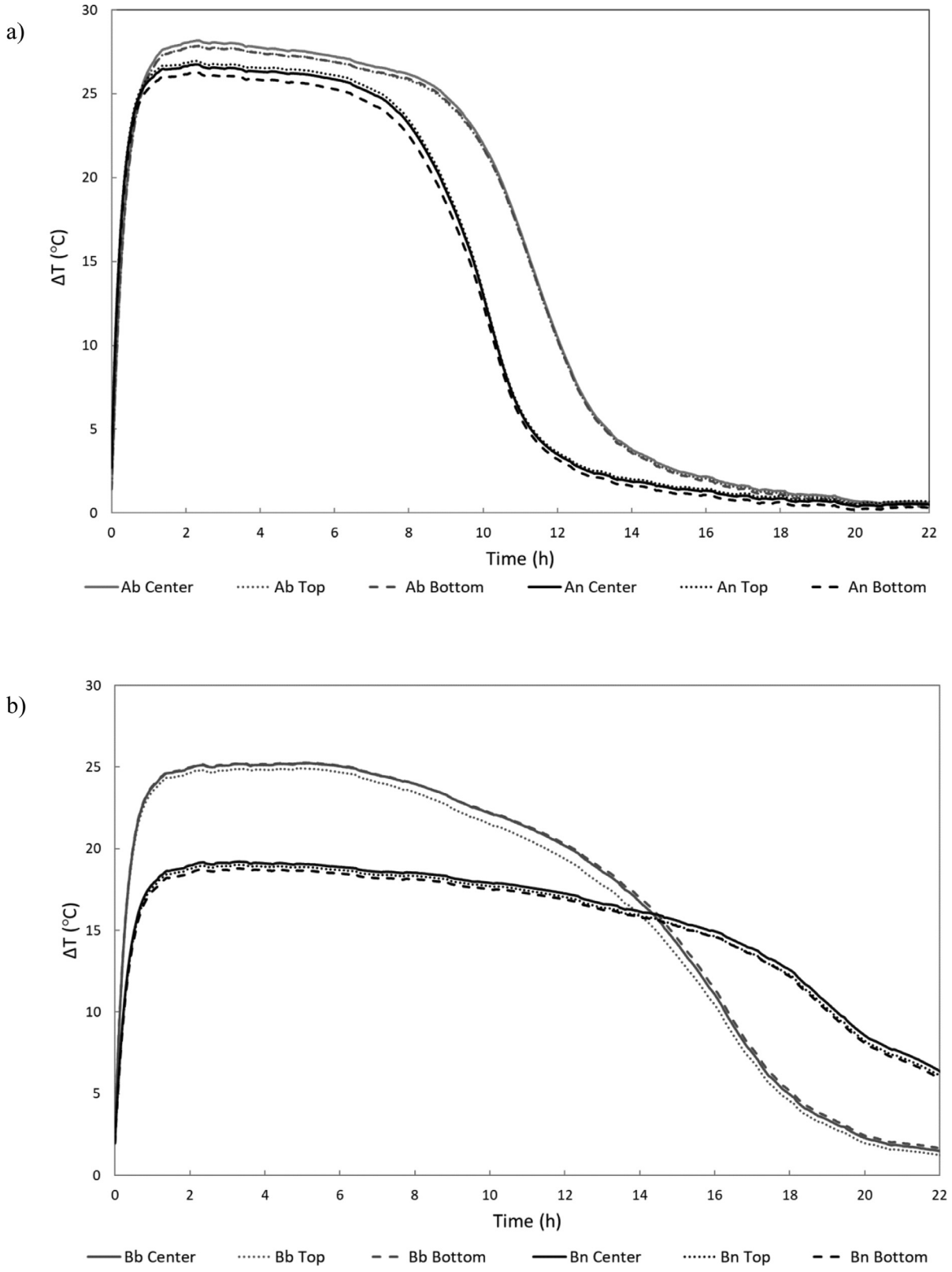

Fig. 9. ΔT trend comparison between heat wraps of the same brand: (a) A_b and A_n; (b) B_b and B_n. The 3 signatures from the thermocouples at the sampling locations on foil-bottom surface (center, bottom and top) are shown.

Table 2
ΔT_{max}, t_{max} and t_{eff} for all tested heat wraps for LBP treatment with batch-based statistical analysis.

Brand	Batch	Sample	ΔT_{max} (°C)	t_{max} (h)	t_{eff} (h)
A	1	1	23.97	2.49	13.65
		2	23.96	2.60	13.73
		3	24.34	2.60	13.73
		4	25.67	2.69	13.01
		5	24.89	2.83	13.45
		Mean *M*	24.56	2.64	13.51
		SD	0.65	0.11	0.27
A	2	1	27.98	2.34	11.41
		2	23.75	2.40	13.69
		3	25.42	2.52	12.53
		4	23.69	2.83	13.62
		5	23.66	2.44	13.66
		Mean *M*	24.90	2.51	12.98
		SD	1.68	0.17	0.90
A	3	1	26.16	2.70	12.55
		2	25.47	2.83	13.08
		3	23.94	2.53	14.25
		4	23.61	2.58	14.13
		5	25.94	2.33	13.27
		Mean *M*	25.03	2.59	13.46
		SD	1.05	0.17	0.64
B	1	1	24.59	3.67	16.55
		2	25.65	6.00	16.19
		3	24.57	4.27	16.54
		4	24.32	4.40	15.64
		5	23.90	6.64	16.95
		Mean *M*	24.61	4.99	16.37
		SD	0.58	1.13	0.44
B	2	1	25.15	4.96	15.50
		2	26.75	2.61	14.39
		3	24.65	4.09	15.93
		4	24.43	3.04	16.93
		5	25.75	3.98	15.77
		Mean *M*	25.35	3.73	15.70
		SD	0.84	0.83	0.82
B	3	1	23.38	4.67	17.05
		2	23.95	6.24	16.27
		3	24.29	4.79	15.64
		4	25.52	5.19	14.49
		5	24.85	3.82	15.32
		Mean *M*	24.40	4.94	15.76
		SD	0.74	0.79	0.87

Table 3
ΔT_{max}, t_{max} and t_{eff} for all tested heat wraps for NP treatment with batch-based statistical analysis.

Brand	Batch	Sample	ΔT_{max} (°C)	t_{max} (h)	t_{eff} (h)
A	1	1	26.66	2.27	10.57
		2	28.20	2.43	9.62
		3	26.33	2.23	10.50
		4	29.32	1.59	8.73
		5	28.35	2.15	9.53
		Mean *M*	27.77	2.13	9.79
		SD	1.12	0.29	0.68
A	2	1	26.67	2.26	9.94
		2	25.45	1.98	10.44
		3	26.31	2.09	9.77
		4	25.74	2.60	9.83
		5	26.86	1.56	9.78
		Mean *M*	26.21	2.10	9.95
		SD	0.54	0.34	0.25
A	3	1	25.08	2.83	11.07
		2	25.79	2.43	10.35
		3	25.46	2.33	10.95
		4	27.32	2.59	9.84
		5	27.79	2.13	9.65
		Mean *M*	26.29	2.46	10.37
		SD	1.07	0.24	0.57
B	1	1	20.45	5.60	19.55
		2	20.81	4.76	17.32
		3	21.92	4.73	16.24
		4	20.62	4.53	17.82
		5	20.07	5.11	19.36
		Mean *M*	20.78	4.95	18.06
		SD	0.62	0.37	1.25
B	2	1	19.01	3.32	19.37
		2	19.82	4.81	19.50
		3	18.90	3.49	19.95
		4	20.11	4.91	19.36
		5	19.91	4.11	18.93
		Mean *M*	19.55	4.13	19.42
		SD	0.50	0.66	0.33
B	3	1	20.48	3.29	21.50
		2	19.87	4.70	20.69
		3	20.40	5.28	19.50
		4	20.51	4.34	18.90
		5	20.09	3.54	20.54
		Mean *M*	20.27	4.23	20.23
		SD	0.25	0.73	0.92

treatment, ΔT_{max} is quite similar over *A* and *B* batches, whereas *B* types feature overall longer t_{eff} values, which hints at longer lifetime. With regard to neck pain treatment, ΔT_{max} is higher in *A* type batches than in the *B* ones, whereas these latter show remarkably longer t_{eff} values. In general, it appears that higher ΔT_{max} values correspond to lower t_{eff} values: even though there are a few cases in contrast with this observation, a correlation between maximum wrap/foil interface temperature and effective duration of the treatment seems to hold. The heat rate released per unit area is proportional to ΔT and the total released energy can be calculated by integrating heat rate over the heat-wrap lifetime. Ultimately, the area subtended by ΔT curve is proportional to the total energy per unit area released by chemical reactions and embedded in the materials contained within each heat wrap. This energy depends on the amount of reacting matter and on its distribution over the wrap active surface (e.g., cells, pockets), which substantiate the relationship with heat-wrap geometry and configuration: the energy-release trend may vary over the tested heat-wrap types by the different kinetics of chemo-physical reactions, ultimately governed by the materials involved and the physical structure of the product.

Some *in vivo* studies investigated the increase of skin and intramuscle temperatures as different heat-wrap types were applied [21,50] and previous research has shown that mild heating may lead to pain reduction, improved circulation and reduction of muscle spasm [21,50,51]. However, those findings do not allow identifying an optimum for heat-therapy duration, nor do they quantify an optimum temperature a heat wrap should achieve to perform well. Moreover, the inherent physiological differences between LBP and NP in terms of muscular response to heat suggest that a unique critical value for ΔT_{max} or t_{eff} may not apply, especially in the context of variable patient responses. So, the quantitative analysis proposed here serves as a comparison between heat wraps, while it does not determine which yields the most effective treatment.

Table 4
F-value, *F*-critical value and *p*-value by ANOVA for each set of batches; level of significance α equal to 0.01.

	F-value	*F*-critical value	*p*-value
A_b type batches	0.16	6.93	0.87
B_b type batches	1.89	6.93	0.24
A_n type batches	3.49	6.93	0.04
B_n type batches	6.5	6.93	0.04

The outcomes of the ANOVA statistical analysis on ΔT values over all 3 tested batches for each heat-wrap type are reported in Table 4. No statistically significant difference between batches of the same type was found, even with an imposed high level of significance ($\alpha = 0.01$). The calculated *F*-value is lower than the *F*-critical value in the whole set of analyzed batches. Consequently, *p*-values are higher than α in all cases. So, ΔT over the 3 batches belonging to the same type and within each batch shows no

statistical difference, hence the high repeatability of the experimental procedure.

5. Conclusions

This study describes a methodology and an experimental setup developed to evaluate quantitatively the transient thermal behavior of heat wraps for thermotherapy. The test rig is simple and virtually free from possible biases due to variability of ambient conditions or to radiative and convective contributions within the test chamber. The measuring system is very mildly intrusive and yields fast response to the heat transferred from the heat-wrap active surface to the reference body: an evaluation of the average surface effect is directly achieved, rather than calculating it from energy-release datasets (e.g., by calorimetric measurements). The proposed method does not involve experiments on users, so the uncertainty inherently related with each individual's reaction to the treatment is removed. Moreover, tests performed by the proposed approach can be faster than *in vivo* studies, allowing to achieve a statistically relevant dataset in a shorter time.

The procedure was validated by a preliminary infrared-thermography assessment and then applied to a number of heat wraps for both LBP and NP treatment. The statistical analysis – including ANOVA – performed on the whole dataset also supported robustness and repeatability of the proposed approach, since no significant differences arose between tests on the same heat-wrap type.

Heat-release trends and parameters of interest in comparing heat wraps for LBP and NP treatment resulted from data analysis. Heat-release rate exhibited a trend qualitatively common to all the investigated types: an initial rapid growth followed by an almost stationary phase, then a decay and finally an asymptotic phase as reactions end. The quantitative differences between heat-wrap types were summarized into maximum achieved temperature, time to reach it and effective lifetime. Overall, it appears the bigger the first one, the shorter the last one; this relationship appears founded on the materials participating in the chemical reactions within heat wraps and on heat-wrap physical configuration. Further studies are suggested to investigate chemical and design factors influencing this relationship. In this regard, the method proposed here can act as a reference to compare heat-wrap performance.

Acknowledgments

The authors wish to thank Dr. A. Libbra and R. Formentini (Università degli Studi di Modena e Reggio Emilia, Italy) for their help and technical advising. The fruitful discussions with R. Schina, M. Alemanni and G. Amici (Bayer S.p.A., Italy) are also acknowledged. This study is part of a research program supported by Bayer S.p.A., Italy. The authors declare no competing interests; no ethical approval is required for the research presented in this work.

References

[1] Anderson GBJ. The epidemiology of spinal disorders. In: Fry Moyer JW, editor. The adult spine: principles and practice. Philadelphia, PA, USA: Lippincott-Raven; 1997. p. 93–141.
[2] Murray CJ, Vos T, Lozano R, Naghavi M, Flaxman AD, Michaud C, et al. Disability-adjusted life years (DALYs) for 291 diseases and injuries in 21 regions, 1990–2010: a systematic analysis for the Global Burden of Disease Study 2010. Lancet 2013;380:2197–223.
[3] Duthey B. Background Paper 6.24 – Low back pain. Priority medicines for Europe and the world–A public health approach to innovation, 6. Geneva, Switzerland: World Health Organization; 2013. p. 24–9.
[4] Fejer R, Kyvik KO, Hartvigsen J. The prevalence of neck pain in the world population: a systematic critical review of the literature. Eur Spine J 2006;15:834–48.
[5] Haldorsen EM, Indahl A, Ursin H. Patients with low back pain not returning to work. A 12 month follow-up study. Spine 1998;23:1202–7.
[6] Maniadakis N, Gray A. The economic burden of back pain in the UK. Pain 2000;84:95–103.
[7] Borghouts JA, Koes BW, Vondeling H, Bouter LM. Cost-of-illness of neck pain in the Netherlands in 1996. Pain 1999;80:629–36.
[8] Côte P, Cassidy JD, Carroll L. The treatment of neck and low back pain: who seeks care? Who goes where? Med Care 2001;39:956–67.
[9] Siegmeth W, Sieberer W. A comparison of the short-term effects of ibuprofen and diclofenac in spondylosis. J Int Med Res 1978;6:369–74.
[10] Blantz RC. Acetaminophen: acute and chronic effects on renal function. Am J Kidney Dis 1996;28:3–6.
[11] Blot WJ, McLaughlin JK. Over-the-counter nonsteroidal anti-inflammatory drugs and risks of gastrointestinal bleeding. J Epidemiol Biostat 2000;5:137–42.
[12] Nadler SF. Nonpharmacologic management of pain. J Am Osteopath Assoc 2004;104:6S–12S.
[13] Nadler SF, Steiner DJ, Erasala GN, Hengehold DA, Abeln SB, Weingand KW. Continuous low-level heatwrap therapy for treating acute nonspecific low back pain. Arch Phys Med Rehabil 2003;84:329–34.
[14] Lloyd A, Scott DA, Akehurst RL, Lurie-Luke E, Jessen J. Cost-effectiveness of low-level heat wrap therapy for low back pain. Value Health 2004;7:413–22.
[15] Petrofsky J, Berk L, Bains G, Khowailed IA, Lee H, Laymon M. The efficacy of sustained heat treatment on Delayed-Onset Muscle Soreness. Clin J Sport Med 2017;27:329–37.
[16] Raleigh G, Rivard R, Fabus S. Air-activated chemical warming devices: effects of oxygen and pressure. Undersea Hyperb Med 2005;32:445–9.
[17] Shaheed CA, Maher CG, Williams KA, McLachlan AJ. Interventions available over the counter and advice for acute low back pain: systematic review and meta-analysis. J Pain 2014;15:2–15.
[18] Nadler SF, Steiner DJ, Erasala GN, Hengehold DA, Hinkle RT, Beth Goodale M, et al. Continuous low-level heat-wrap therapy provides more efficacy than Ibuprofen and acetaminophen for acute low back pain. Spine 2002;27:1012–17.
[19] Nadler SF, Steiner DJ, Erasala GN, Hengehold DA, Abeln SB, Weingand KW. Continuous low-level heatwrap therapy for treating acute nonspecific low back pain. Arch Phys Med Rehabil 2003;84:329–34.
[20] Michlovitz S, Hun L, Erasala GN, Hengehold DA, Weingand KW. Continuous low-level heat wrap therapy is effective for treating wrist pain. Arch Phys Med Rehabil 2004;85:1409–16.
[21] Mayer JM, Mooney V, Matheson LN, Erasala GN, Verna JL, Udermann BE, et al. Continuous low-level heat-wrap therapy for the prevention and early phase treatment of delayed-onset muscle soreness of the low back: a randomized controlled trial. Arch Phys Med Rehabil 2006;87:1310–17.
[22] Trowbridge CA, Draper DO, Feland JB, Jutte LS, Eggett DL. Paraspinal musculature and skin temperature changes: comparing the ThermaCare HeatWrap, the Johnson & Johnson Back Plaster, and the ABC Warme-Pflaster. J Orthop Sports Phys Ther 2004;34:549–58.
[23] Tao X, Bernacki EJ. Randomized clinical trial of continuous low-level heat therapy for acute muscular low back pain in the workplace. J Occup Environ Med 2005;47:1298–306.
[24] Draper DO, Ty Hopkins J. Increased intramuscular and intracapsular temperature via ThermaCare® Knee Wrap application. Med Sci Monit 2008(14):PI7–PI11.
[25] Cramer H, Baumgarten C, Choi K-E, Lauche R, Saha FJ, Musial F, et al. Thermotherapy self-treatment for neck pain relief – A randomized controlled trial. Eur J Integr Med 2012;4:371–8.
[26] Rosenberg N, Gelijns AC, Dawkins H. The changing nature of medical technology development. In: Rosenberg N, Gelijns AC, Dawkins H, editors. Sources of medical technology: universities and industry. Washington, DC, USA: The National Academies Press; 1995. p. 3–14.
[27] Chien S, Bashir R, Nerem RM, Pettigrew R. Engineering as a new frontier for translational medicine. Sci Transl Med 2015(7):281fs13. doi:10.1126/scitranslmed.aaa4325.
[28] Ezzat MA, El-Bary AA, Al-Sowayan NS. Tissue responses to fractional transient heating with sinusoidal heat flux condition on skin surface. Anim Sci J 2016;87:1304–11.
[29] Hildebrandt C, Raschner C, Ammer K. An overview of recent application of medical infrared thermography in sports medicine in Austria. Sensors 2010;10:4700–15.
[30] Necati Özişik M. Boundary value problems of heat conduction. 2nd ed. Mineola, NY, USA: Dover Publications; 2002.
[31] Ezzat MA. Free convection effects on extracellular fluid in the presence of a transverse magnetic field. Appl Math Comput 2004;15:455–82.
[32] Ezzat MA. Free convection flow of conducting micropolar fluid with thermal relaxation including heat sources. J Appl Math 2004;4:271–92.
[33] Incropera FP, DeWitt D, Bergman TL, Lavine AS. Fundamentals of heat and mass transfer. 6th ed. Hoboken, NJ, USA: Wiley; 2007.
[34] Wolkoff P. Indoor air humidity, air quality, and health – An overview. Int J Hyg Environ Health 2018;221:376–90.
[35] Standard 55-2017: thermal environmental conditions for human occupancy. In: Proceedings of the refrigerating and air-conditioning engineers, Atlanta, GA, USA. ASHRAE – American Society of Heating; 2017.
[36] Young HD, Freedman RA. University physics with modern physics. 13th ed. Hoboken, NJ, USA: Pearson Education; 2014.
[37] Ezzat MA, Al Sowayan NS, Al-Muhiameed ZIA, Ezzat SM. Fractional modelling of Pennes' bioheat transfer equation. Heat Mass Transf 2014;50:907–14.
[38] Tarozzi L, Muscio A, Tartarini P. Experimental tests of dropwise cooling on infrared-transparent media. Exp Therm Fluid Sci 2007;31:857–65.

[39] Tartarini P, Corticelli MA, Santangelo PE. Experimental and numerical analysis of droplet cooling. In: Proceedings of the 14th international heat transfer conference, vol. 6; 2010. p. 677–85.
[40] Orlandini S, Moretti G, Corticelli MA, Santangelo PE, Capra A, Rivola R, et al. Evaluation of flow direction methods against field observations of overland flow dispersion. Water Resour Res 2012;48:W10523.
[41] Santangelo PE, Corticelli MA, Tartarini P. Spray cooling by gently-deposited droplets: experiments and modeling of heat-transfer mechanisms. In: Proceedings of 15th International Heat Transfer Conference; 2014. IHTC15-8367.
[42] Santangelo PE, Allesina G, Bolelli G, Lusvarghi L, Matikainen V, Vuoristo P. Infrared thermography as a Non-Destructive Testing solution for thermal spray metal coatings. J Therm Spray Technol 2017;26:1982–93.
[43] Santangelo PE, Tartarini P. Effects of load variation and purge cycles on the efficiency of Polymer Electrolyte Membrane Fuel Cells for stationary applications. J Renew Sustain Energy 2018;10:014301.
[44] Santangelo PE, Corticelli MA, Tartarini P. Experimental and numerical analysis of thermal interaction between two droplets in spray cooling of heated surfaces. Heat Transf Eng 2018;39:217–28.
[45] Santangelo PE, Tartarini P. Full-scale experiments of fire suppression in high-hazard storages: a temperature-based analysis of water-mist systems. Appl Therm Eng 2012;45-46:99–107.
[46] Santangelo PE, Tarozzi L, Tartarini P. Full-scale experiments of fire control and suppression in enclosed car parks: a comparison between sprinkler and water-mist systems. Fire Technol 2016;52:1369–407.
[47] Kim H-Y. Analysis of variance (ANOVA) comparing means of more than two groups. Restor Dent Endod 2014;39:74–7.
[48] Fisher RA. A mathematical examination of the methods of determining the accuracy of an observation by mean error and by the mean square error. Mon Not R Astron Soc 1920;80:758–70.
[49] Hahn GJ, Shapiro SS. Statistical models in engineering. Hoboken, NJ, USA: Wiley; 1994.
[50] Draper DO, Harris ST, Schulthies SS, Durrant E, Ricard MD, Knight KL. Hot-pack and 1-MHz ultrasound treatments have an additive effect on muscle temperature increase. J Athl Train 1998;33:21–4.
[51] Bélanger A-Y. Evidence-based guide to therapeutic physical agents. Baltimore, MD, USA: Lippincott Williams & Wilkins; 2002.